LABORATORY INCUBATIONS OF MACONDO OIL-DERIVED HYDROCARBONS IN ALABAMA SALT MARSH SEDIMENTS AND WATER

by

DANIEL JAMES FIELDS

YUEHAN LU, COMMITTEE CHAIR

ALBERTO PEREZ-HUERTA
ROBERT FINDLAY
RONA DONAHOE

A THESIS

Submitted in partial fulfillment of the requirements
for the degree of Master of Science in the
Department of Geological Sciences
in the Graduate School of
The University of Alabama

TUSCALOOSA, ALABAMA

2013

ABSTRACT

In order to better understand the impact of the *BP Deepwater Horizon* and future oil spills on the Gulf of Mexico coast this study assesses the variation of alkanes and polycyclic aromatic hydrocarbons (PAH) in coastal sediments and water. 500g of Sediment and water from Bayou La Batre, Alabama was spiked with 10g Macondo oil for a time series experiment with sampling points at 0, 6, 12, 24, 48, 168, and 336 hours. Sediment and water were also spiked with 0.2g, 2g, 10g, 20g and 50g Macondo oil and were incubated for 21 days for a concentration variation experiment. The composition and concentrations of alkanes and PAHs in the sediments and the concentrations of dissolved inorganic nitrogen and phosphorous and dissolved organic carbon were characterized.

Results from the time series experiment show 54.6% total alkanes in sediments were lost within the first six hours and 71.5% were lost after 14 days. Total PAHs decreased by 90.1% within the first six hours and did not show apparent decreases afterwards. The loss of hydrocarbons in the sediments may be attributed to microbial degradation. Low molecular weight (≤ C17) alkanes were preferentially degraded over high molecular weight (> C17) alkanes during the first 24 hours, whereas normal alkanes were not preferentially degraded over isoprenoid alkanes. The high degradation rates of hydrocarbons in the first 12 hours were attributed to aerobic microbial degradation rates of hydrocarbons; the decreases in the loss rates after hour 12 were perhaps due to oxygen depletion in the microcosms. The oxygen depletion was supported by the elevated iron concentration in seawater after 168 hours that indicated anaerobic microbial respiration using Fe (III) as an electron acceptor. However, the concentration of dissolved nitrate and ammonium did not show evident patterns over the course of the incubation, providing no evidence that nitrate was used by microbes as an electron

acceptor during anaerobic microbial respiration. Dissolved organic carbon (DOC) concentration continuously decreased until reaching the ambient seawater concentration, indicating an active microbial degradation of oil-derived hydrocarbons that were dissolved in the seawater.

In the concentration variation experiment, sterilized controls with 0.2g and 20g of oil treatment had much higher concentrations of saturated alkanes in the sediments than corresponding non-sterilized microcosms with *in situ* microbial community left intact. However, the microcosms with 10g and 50g of oil treatment did not show reduced concentration of hydrocarbons in the sediments relative to their non-sterilized counterparts. Similarly, variable patterns appeared from the comparison of the dissolved organic carbon concentrations between non-sterilized microcosms *vs.* sterile microcosms treated with the same amount of oil. Therefore, data from the concentration variation experiment provided inconclusive evidence that the *in situ* microbial community degraded oil-derived alkanes in sediments and seawater of the microcosms.

DEDICATION

This thesis is dedicated to my wife, Emily, who pulled me through the stress and struggles of this two year journey, and who never let me doubt myself. She has been with me every step of the way, and I could not have completed this manuscript without her.

LIST OF ABBREVIATIONS AND SYMBOLS

GOM	Gulf of Mexico
SD	standard deviation
PAH	polycyclic aromatic hydrocarbon
DOC	dissolved organic carbon
TOC	total organic carbon
TN	total nitrogen
C	carbon
N	nitrogen
PDB	Pee Dee Belemnite
LMW	low molecular weight
HMW	high molecular weight
NSC	non-sterile control without oil treatment
SC	sterile control
K_{ow}	octonal-water partition coefficient
WS	water solubility
uM	micromolar
m	meter

cm	centimeter
mL	milliliter
g	gram
ppm	parts per million
ppb	parts per billion
rpm	rotations per minute
hr	hour
mg/L	milligrams per liter
UHP	ultra-high purity
GC	gas chromatograph
GC-MS	gas chromatograph-mass spectrometer
log	logarithm
<	less than
≥	greater than or equal to

ACKNOWLEDGMENTS

I would like to thank all of the colleagues, friends, and faculty members who have helped me along the way of creating this manuscript. First, I would like to thank Yuehan Lu, my committee chair, who has been an invaluable resource to me during this process. I am greatly indebted to Yuehan for teaching me lab techniques, and lending much of her time and effort to help me with this project. I would also like to thank my committee members, Rona Donahoe, Alberto Perez-Huerta and Robert Findlay, for their insightful questions and guidance during the research process. Also, a special thanks to Rona Donahoe and Erika Rentschler for allowing me use of Rona's lab and the sharing of their samples and Robert Findlay for use of his lab and equipment. Without this, my project would not have been possible. I would also like to thank Laura Linn and my colleagues at the Dauphin Island Sea Lab for the use of their facilities during experimentation. I am also indebted to Joe Lambert for instruction and use of lab equipment in the Alabama Stable Isotope Laboratory. Finally, I would like to thank Yuchi Qin, Joey Cardosi, and Andrea Jaegge for their generous help in the lab.

CONTENTS

LIST OF TABLES

LIST OF FIGURES

CHAPTER 1

INTRODUCTION

The BP *Deepwater Horizon* spill, occurring April 20, 2010, is the largest marine oil spill accident in human history. During this spill, 4.9 million barrels was estimated to have been released (Atlas and Hazen, 2011). The Oil Budget calculator estimated that 50% of the oil was removed via skimming, burning or capturing, or evaporation (Atlas and Hazen, 2011). Of the remaining 50% of oil, 24% was physically or chemically dispersed, and 26% is unaccounted for (Atlas and Hazen, 2011). Although the shores of Alabama were impacted by the BP spill, very little is known about the degradation of oil in Alabama's coastal environments. To determine this, we must have an understanding of the chemical composition of crude oil, specifically the spilled Macondo oil.

Crude oil is primarily composed of hydrocarbons with various molecular weights and structures. Aliphatic hydrocarbons include alkanes, which can be straight chained (normal) or branched. When eluted in a gas chromatogram a wide range of crude oils have a carbon number range of C_8-C_{40}, including normal and branched alkanes (Wang et al., 1999). Hydrocarbons with less than eight carbons tend to evaporate during the acquisition or extraction phase of crude oil. Alkane composition varies among different oils and determines the density of crude oil. Wang et al. (1999) demonstrates that jet fuel is abundant in C_9-C_{16} alkanes, whereas diesel fuel can range in composition from C_8-C_{40} alkanes. Pristane and Phytane are isoprenoid (branched) alkanes with C_{19} and C_{20}, respectively and are often the most abundant isoprenoid hydrocarbons in oil. The alkane composition of oil provides information about weathering degrees of crude oil. Since

short-chain (< C_{17}) alkanes are preferred by bacteria and are relatively more volatile than their long-chain counterparts, their absences indicates oil has been weathered to a greater extent (Ezra et al., 2000; Wu et al., 2001; Atlas and Philp, 2005). For example, the ratios of n-C_{17}:Pristane and n-C_{18}:Phytane can be used to determine the degree of weathering/biodegradation of fresh to mildly weathered crude oil (Wang et al., 1999). A decreasing trend of these ratios over time supports that normal alkanes are preferentially degraded over branched alkanes.

Polycyclic aromatic hydrocarbons (PAHs) are a component of crude oil that is toxic to marine organisms and humans. PAHs have been shown to be carcinogenic to humans, and both carcinogenic and mutagenic to terrestrial and aquatic organisms (Ke et al., 2001; Wu et al., 2001; Arzayus et al., 2002; Countway et al., 2003; Yamada et al., 2003; Banjoo and Nelson, 2005). The structure of polycyclic aromatic hydrocarbons includes 2 or more 5-6 member carbon rings fused together (Irwin, 1997). Low molecular weight (LMW) PAHs include structures with 2-3 fused rings and high molecular weight (HMW) PAHs include structures with 4 or greater fused rings.

The spilled Macondo oil was light Louisiana crude with an API gravity of 35.2 (Atlas and Hazen 2011). The liquid hydrocarbon content extracted from the Macondo oil is 74% alkanes, 16% PAHs, and 10% polar hydrocarbons (Reddy et al., 2011). Macondo oil alkanes range in carbon number from C_1 to C_{33} (Reddy et al., 2011). Alkanes from C_6 to C_{11} are the most abundant components in the liquid oil, ranging from 0.011 to 0.012 g g^{-1} of oil. PAHs in the liquid oil range from two to five rings and exist as Naphthalene, Dibenzothiophene, Fluorene, Phenanthrene, Fluoranthene, Pyrene, Chrysene, Anthracene and Benz[a]anthracene. The concentrations of these PAHs range from 0.000006 to 0.0004 g g^{-1} of oil (Reddy et al., 2011). The polar hydrocarbons in the liquid oil contain oxygen, nitrogen, and sulfur and span a large

molecular weight range (Reddy et al., 2011). When crude oil is released into the environment, weathering and degradation occur immediately.

Degradation of oil occurs in several different ways, including microbial degradation, physical and chemical dispersion, evaporation, photooxidation, dissolution, combustion, and skimming (Atlas and Hazen, 2011).

Microbial degradation can be carried out by many groups of bacteria, archaea, and fungi, which are able to metabolize aliphatic and aromatic hydrocarbons in oil (Atlas and Hazen, 2011). Of these oil degraders, bacteria are the most important, particularly those belonging to the genera *Alcanivorax, Cycloclasticus, Marinobacter, Neptunomonas, Oleiphilus, Oleispira, Thalssolituus* (Miralles et al., 2007). The rates of hydrocarbon degradation by bacteria can be limited by availability of oxygen, nitrates (NO_3^-), phosphates (PO_4^{3-}), and iron (Fe) (Atlas and Hazen, 2011). Aerobic degradation of hydrocarbons by bacteria begins with dioxygenase enzymes inserting O_2 into the structure which yields CO_2 and H_2O, while anaerobic degradation of hydrocarbons occurs with the availability of various electronic acceptors such as nitrate and oxidized iron (Atlas and Philp, 2005). As a result, microbial degradation of hydrocarbons has been proven to be an integral strategy of oil spill cleanup efforts (Leahy and Colwell, 1990; Volkman et al., 1984; Hostettler and Kvenvolden, 1994; Boopathy et al., 2012; Natter et al., 2012). For example, the main remediation strategy of the *Exxon Valdez* spill of 1989 was biostimulation of the in-situ microbial community using fertilizers to increase the rate of oil degradation on the shores of Prince William Sound (Atlas and Hazen 2011).

Chemical dispersion is one important method widely used for cleaning marine oil spills (Atlas and Philp, 2005). Hydrocarbons are hydrophobic and thus are not dissolved in water but form a separate phase, also known as non-aqueous phase liquid (NAPL). Consequently,

biodegradation is limited at the hydrocarbon-water interface. Dispersants can increase the surface area of oil by forming micelles and creating oil droplets, which subsequently increases the contact areas between oil and microbes (Atlas and Hazen, 2011). The increased surface area of the oil may result in higher availability for microbes to degrade the oil. The formation of droplets also allows the oil to be dispersed throughout the water column instead of forming a slick on the waters' surface. During the BP spill, an unprecedented amount of the dispersant COREXIT 9500 was used, much of it in deep water next to the wellhead (Atlas and Hazen, 2011).

Photooxidation and evaporation of oil occur when an oil slick forms, exposing it to sunlight and the atmosphere. It is estimated that 25% of the oil in the BP spill was degraded in this way (Atlas and Hazen, 2011). Short-chained aliphatic and LMW PAHs are susceptible to complete evaporation within 2 to 3 days of being exposed to the atmosphere (Wang et al., 1999); whereas HMW PAHs, particularly with increasing alkyl substitution, are susceptible to photooxidation (Garrett et al., 1998).

Although some Macondo oil from the BP spill reached Alabama coastal waters and beaches, including Bon Secour (OSAT-2 Annex B, 2011), Walker Island (Natter et al., 2012), and Mobile Bay (Atlas and Hazen, 2011), little is known about the fate of these oil-derived compounds in Alabama coastal zones. One of the most concerning area is salt marshes, which are often characterized by low dissolved oxygen content and accumulation of great amounts of organic matter. It is not unusual that oil compounds accumulate in salt marshes after an oil spill (Boopathy et al., 2012; Natter et al., 2012). For example, Oudot and Chaillan (2010) determined that the Amoco-Cadiz spill still affects salt marshes of Ile Grande on the French Coast after 23 years. Salt marshes are however both ecologically and economically important. They provide

homes to many species of plants and animals, including grasses, fish, birds, insects, rodents, and benthic organisms and act as a major source of business (King and Lester, 1995).

The objective of the present study was to better understand the fate of hydrocarbons from Macondo oil in Alabama salt marsh sediments and seawater. We hypothesized that: 1) the majority of hydrocarbon compounds may be degraded by microbes in salt marsh sediments and water and 2) the degradation rate is controlled by oxygen and nutrient availability to microbes as well as the structure of hydrocarbon compounds. In order to test these hypotheses, microcosm experiments simulating oil loss in both sediment and seawater collected from Bayou La Batre, Alabama were performed. First, a time series experiment was conducted with 20 microcosms filled with sediment and seawater and spiked with 10g Macondo oil to understand *in situ* microbial degradation of hydrocarbons for a 14 day incubation. Second, a concentration variation experiment was conducted with 18 microcosms filled with sediment and seawater from the same location and spiked with 0.2g, 2g, 10g, 20g and 50g of Macondo oil for a 21 day incubation to determine the effects of various hydrocarbon concentrations on *in situ* microbial degradation.

CHAPTER 2

METHODOLOGY

2.1 SITE DESCRIPTION

Seawater and sediment samples were collected near a salt marsh located in Bayou La Batre, Alabama (30.38°N, 88.30°W, Fig. 1) on March 17, 2011 (for the time series experiment described below) and September 12, 2011 (for the concentration variation experiment described below). Bayou La Batre is located in the Gulf Coastal Plain, ~10 miles west of Mobile Bay. The salt marsh is characterized by low, swampy areas with various grass vegetation. The pH of the sampled water was 7.70, with a total alkalinity of 83.07mg of $CaCO_3$/L (Rentschler, 2013). Sediment of this area is made up of inorganic clays, poorly-sorted sands, silty-sand, and sandy-clay (Rentschler, 2013).

2.2 SAMPLE COLLECTION

All containers and sampling equipment that were in direct contact with water samples were either combusted at 450˚C for 5 hours (glass materials), or acid soaked (10% HCl or 10% HNO_3) and thoroughly rinsed with Milli-Q water (plastic materials). Seawater and sediment samples were collected 6-9 meters from shore (1 meter depth). Water was collected under the water's surface using polypropylene bottles and the upper 15-30 cm of sediment was collected into a 5 gallon plastic bucket. All samples were put on ice during transportation to the lab, where they were refrigerated in the dark up to 18 days until the microcosm experiments were conducted.

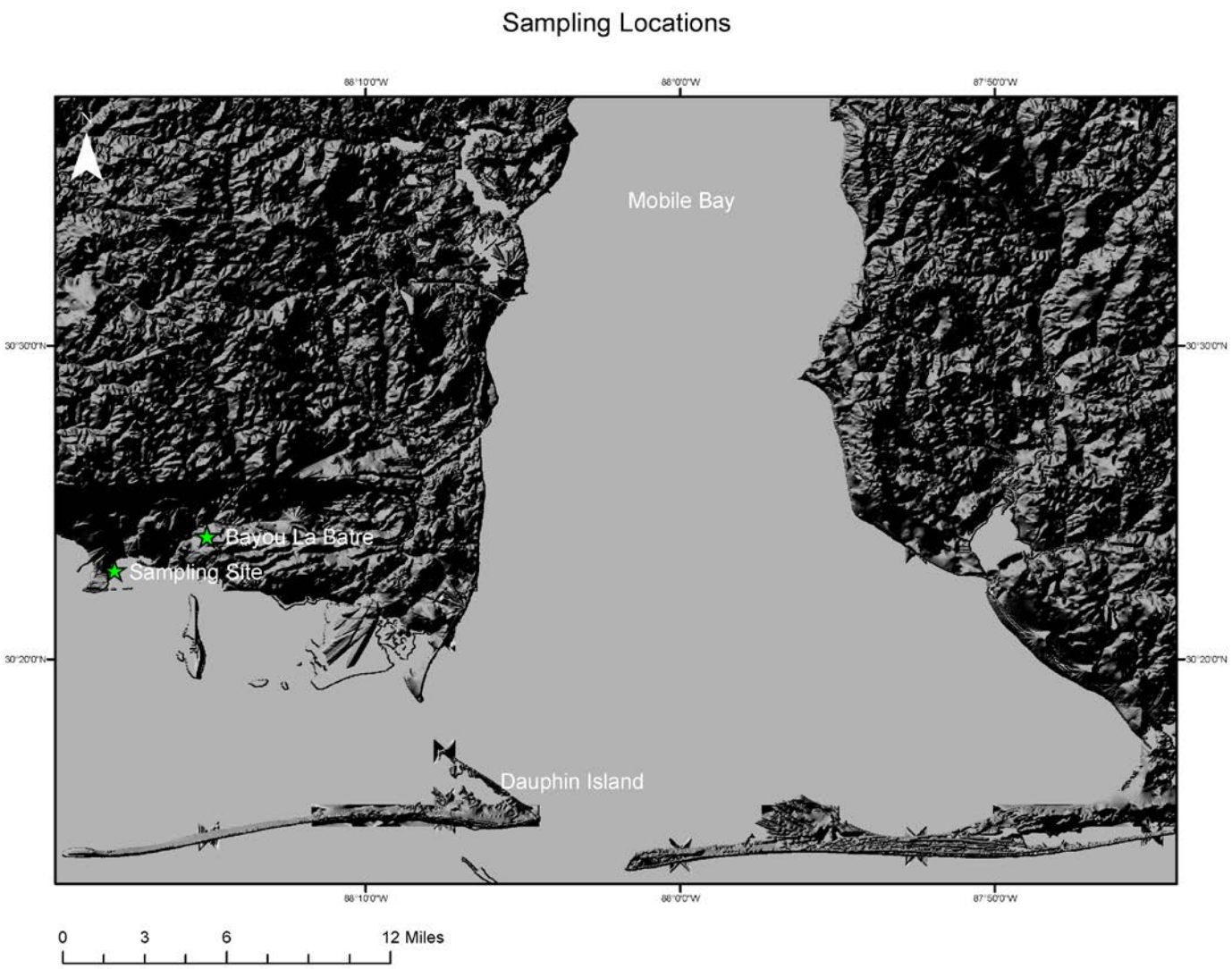

Figure 1: Map featuring the sampling location

2.3 TIME SERIES EXPERIEMENT

Twenty 500 mL glass jars with Teflon-lined lids were each filled with 326.94 g wet sediment (mass equivalent to 200 g dry sediment) and 173.06 g seawater. Control samples consisted of sterile controls (SC) and non-sterile control (NSC) that were not treated with oil and sterile controls that were treated with oil. Sterile controls were autoclaved just prior to the experiment. Samples were spiked with 10 grams of Macondo oil (50,000 ppm relative to dry sediment weight) and incubated for two weeks in the dark on a shaker table set to 100 rpm. Two jars were sacrificed at hour 0, 6, 12, 24, 48, 168, and 336. All controls were sacrificed at hour 336.

2.4 CONCENTRATION VARIATION EXPERIMENT

Eighteen 500 mL glass jars were each filled with 281.56 g of sediment (mass equivalent to 200 g dry sediment) and 118.45 g of seawater. Samples and duplicate jars plus their corresponding sterile controls were spiked with 0.2, 2, 10, 20 and 50 grams of Macondo oil (1,000, 10,000, 50,000, 100,000, and 250,000 ppm oil relative to dry sediment, respectively). No oil was added to two types of controls: non-sterile control (NSC) plus duplicate, and one sterile control (SC). The incubation conditions were the same as with the time series and all jars were sacrificed at day 21.

2.5 ELEMENTAL AND STABLE ISOTOPES OF BULK SEDIMENTS

Sediment samples were freeze-dried and ground to fine powders using a mortar and pestle. $CaCO_3$ was removed by concentrated sulfuric acid prior to the analyses of total organic carbon (TOC, wt%), total nitrogen (TN, wt%), $\delta^{13}C_{org}$ (‰) and $\delta^{15}N$ (‰) using elemental analysis-isotope ratio mass spectrometry (EA-IRMS) flow through system at the Alabama Stable Isotope Laboratory in the Department of Geological Sciences at The University of Alabama.

2.6 HYDROCARBON DETERMINATION IN SEDIMENTS

After incubation, water and sediment within the samples were separated. Water was collected by siphoning the upper liquid layer before and after centrifuging sediments at 750 rpm for 20 minutes. The water samples were then filtered through 0.45 micron nylon membrane filters and stored frozen until analysis for dissolved organic carbon (DOC) and nutrients. Sediment samples were homogenized by stirring and then stored frozen in glass jars prior to hydrocarbon analysis.

Hydrocarbon extraction followed the method described in Risdon et al. (2008) with minor modification. Approximately 6 grams of the sediment were mixed with Hydromatrix (Agilent Technologies) to remove water. n-Hexadecane-d34 ($C_{16}D_{34}$) and phenanthrene-d10 were added as surrogates to the samples prior to the extraction. Samples were then ultrasonically extracted with 4mL Acetone for 2 minutes at 20 °C to ensure a thorough mixture between the sediments and the surrogates. 20mL acetone:hexane (1:1, vol:vol) and was then added to the samples, ultrasonically extracted for 10 minutes at 20 ºC and stored in fridge overnight. Short copper ribbon was used to remove sulfur during the extraction process.

Samples were extracted ultrasonically again for 20 minutes at 20 ºC before the liquid portion of the samples was collected with disposable pipettes and concentrated with an ultra high purity (UHP) nitrogen stream. 3 mL of acetone, 5 mL of hexane, 4 mL of Milli-Q water and a spatula of sodium chloride were added to the extracts, manually shaken for 30 seconds, and allowed to settle for 20 minutes. The top hexane layer was siphoned via disposable pipette as the hydrocarbon fraction and the more polar compounds dissolved in the lower acetone and water layer were discarded. The hydrocarbon fraction was then separated by silica column

chromatography into aliphatic and aromatic hydrocarbon fractions, which were eluted by 10 mL of hexane and 12 mL of dichloromethane respectively.

Aliphatic fractions were quantified and identified using gas chromatography (GC) and gas chromatography-mass spectrometry (GC-MS), respectively. The initial temperature for GC and GC-MS runs was 50°C, held for one minute, followed by a 6°C/min increase until 310°C was reached, then holding for 15 minutes for a total run time of 59 minutes. UHP helium was the carrier gas used at a flow rate of 1.48 mL/min for the GC and GC-MS. The quantification of objective compounds is done by comparing their peak areas to the peak areas of n-Hexadecane-d34. Different instrumental responses for various compounds were corrected by regularly running a standard containing a series of alkane compounds (C_7-C_{40} normal alkanes).

Aromatic components were quantified by their relative retention times and mass spectra and identified by comparison of retention times to a standard with multiple known PAHs using GC and GC-MS, respectively. Phananthrene-d10 was added at a known concentration prior to extraction as an internal standard, from which other aromatic compounds were quantified. Samples were identified under selective ion mode combining mass peaks with retention time. The mass peaks for naphthalene, 2-bromonaphthalene and acenaphthene, fluorene, fluoranthene, and pyrene were 128, 153, 166, 202, and 202, respectively. The retention times were 6.9, 10.7, 12.2, 19.8, 20.6 minutes, respectively. Initial temperature was 50°C, held for one minute, followed by a 20°C/min increase until 140°C was reached, and then a 6°C/min increase until 310°C was reached, holding for 15 minutes for a total run time of 47 minutes.

2.7 WATER SAMPLE DETERMINATION

The DOC concentrations of aqueous samples were determined using a Shimadzu TOC-V_{CPN} Total Organic Carbon Analyzer, with a KHP standard solution for constructing calibration

curves and a consensus seawater reference deep seawater DOC standard (Hansell Laboratory, http://yyy.rsmas.miami.edu/groups/biogeochem/CRM.html) for confirming analytical accuracy. Samples were submitted to the Dauphin Island Sea Lab for nutrient (nitrate + nitrite, nitrite, ammonium, and phosphate) analyses, where they were measured with the Alpkem Rapid Flow Analyzer 2 (RFA/2) which uses continuous flow analysis techniques (Alpkem Manual, 1988).

CHAPTER 3

RESULTS

3.1 BULK SEDIMENT CHARACTERIZATION

TOC content in sediments ranged between 0.88 – 1.45% and TN ranged between 0.08−0.13%, yielding a C:N ratio of 11–11.15. $\delta^{13}C$ values of TOC and $\delta^{15}N$ values varied from -22.0 – -21.4 (‰ PDB) and 3.2 – 4.7 (‰ Air), respectively, falling in the ranges indicating the dominance of marine sources (Mitra et al., 2009).

3.2 TIME SERIES EXPERIEMENT

3.2.1 ALIPHATIC ALKANE LOSS WITH TIME

Hydrocarbon concentrations are expressed as either ppm (mg hydrocarbon/g wet sediment) or ppb (ng hydrocarbon/g wet sediment). For the time series experiment, the non-oiled NSC and the non-oiled SC showed alkanes below detection. The detected alkanes ranged in carbon number 9 through 33, including both normal and isoprenoid alkanes. The data for the oiled SC were not presented because they were dubiously low which may be due to a sampling error. Over the course of the experiment, total alkanes showed significant loss during the first 12 hours and remained relatively stable from hour 12 to 336 (Fig. 2). At hour 12 83.1% total alkanes were lost (Table 1). The average loss rate during the first 6 hours was 222 ppm/hr, slowing to 116 ppm/hr from hour 6 to 12 and further decreasing to 5 ppm/hr thereafter (Table 2).

The pattern of hydrocarbon loss observed here agrees with the patterns of natural organic matter degradation that have been observed in natural seawater and sediment systems (Westrich and Berner, 1984). This pattern may be quantitatively described using a multi-G model (Berner, 1964) below:

$$-dG/dt = \Sigma k_i G_i$$

$$G_t = \sum G_i = (G_1)_0 \exp(-k_1 t) + (G_2)_0 \exp(-k_2 t) + (G_3)_0 \exp(-k_3 t) + \ldots$$

where k_i is the first-order degradation rate constant of fraction i; G_i is the concentration of fraction i and $-dG_t/dt$ is the degradation rate of all fractions.

In our samples, ~87% of total hydrocarbons degraded rapidly within the first 48 hours, accounting for the first, reactive fraction of the oil-derived alkanes (G_1) and yielding k_1 as 0.0373 $hour^{-1}$(RSQ=0.62; Fig. 2). Since the degradation rate decreased rapily after hour 48, the total alkanes between hour 48-336 can be treated as resistant fraction G_2. As only three time points were sampled after hour 48, a reliable value of k_2 cannot be obtained from our experiment.

LMW alkanes decreased faster than HMW alkanes throughout the time series experiment (Fig. 2). By hour 12, LMW alkanes were decreased 89.5%, relative to HMW alkanes that were decreased 76.4% by hour 12 (Table 3). After 168 hours LMW alkanes were decreased by 90.6%, and HMW were decreased by 86%. Using the zero-order degradation rate, the loss rates of LMW and HMW alkanes decreased from 98 and 85 ppm/hr, respectively, between hour 6 and 12 to below detection between hour 168 and 336 (Table 4). Using the multi-G model, k_1 for LMW and HMW alkanes were 0.0389 $hour^{-1}$ and 0.0384 $hour^{-1}$, respectively (Fig. 2).

The loss rates of normal and branched alkanes did not show evident differences, which was shown by that the ratios of C_{17} normal alkane:Pristane (n-C_{17}:Pr) and C_{18} normal alkane:Phytane (n-C_{18}:Ph) did not exhibit an apparent trend over the course of time series experiment (Fig. 2, Table 6).

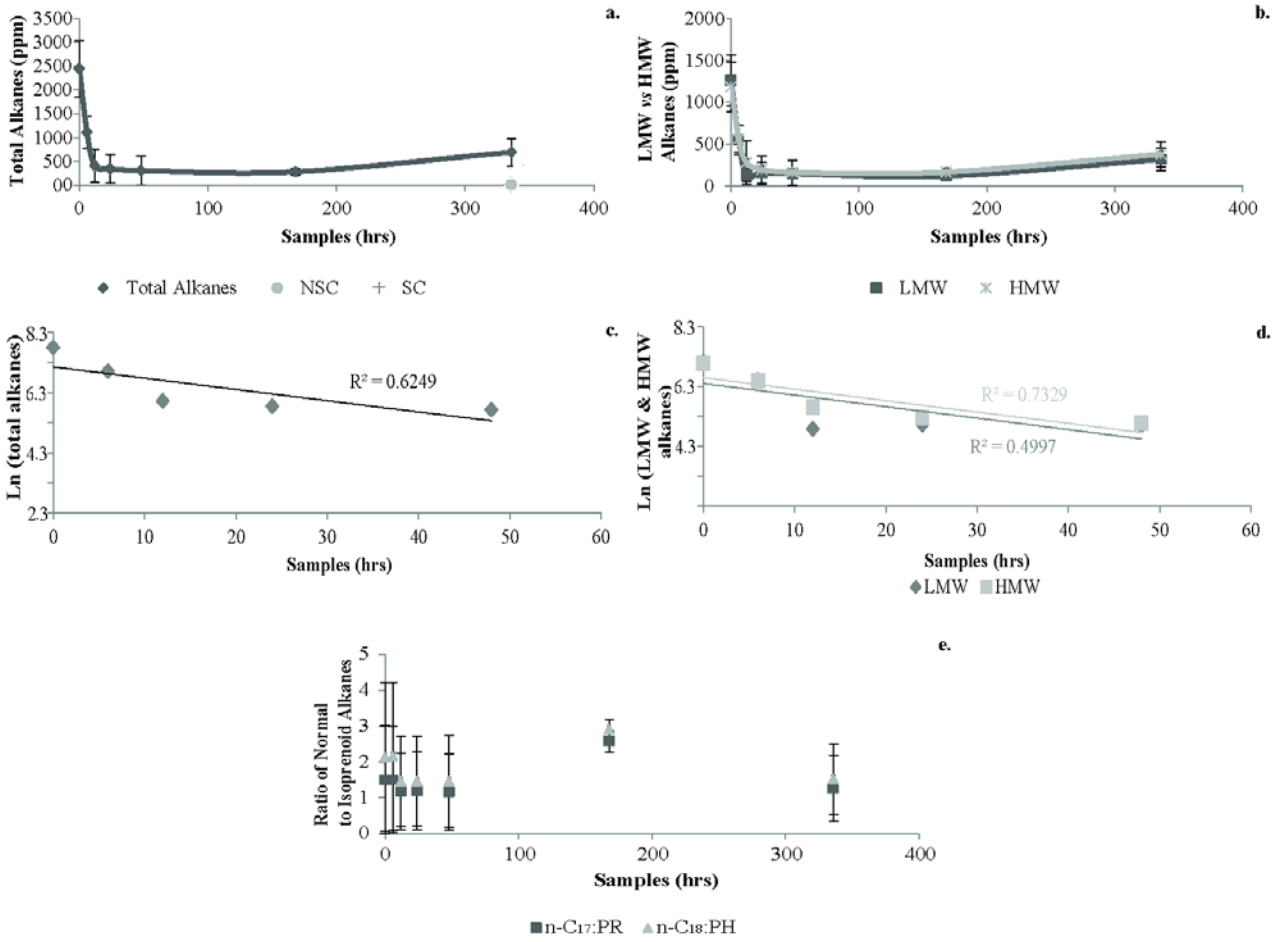

Figure 2: (a) changes in the concentrations of total alkane over the course of the time series experiment; (b) changes in the concentrations of LMS and HMW alkanes over the course of the time series experiment; (c) the first-order degradation fitting line for the changes in total alkanes within the first 48 hours; (d) the first-order degradation fitting line for the changes in LMW and HMW alkanes within the first 48 hours; and (e) changes in the ratio of normal alkane C_{17} to Pristane and normal alkane C_{18} to Phytane over the course of the time series experiment. Error bars represent the SD of data from duplicate incubation bottles.

Table 1: Total alkanes and the % loss over the course of the time series experiment

Sample	**Total Alkanes (ppm in sediments; Mean ± SD)**	**% Loss (Mean)**
NSC (non-oiled)	undetected	n.a.
SC (non-oiled)	undetected	n.a.
Hour 0	2445 ± 597	n.a.
Hour 6	1108 ± 331	54.6
Hour 12	411 ± 339	83.1
Hour 24	346 ± 289	85.8
Hour 48	307 ± 303	87.4
Hour 168	282 ± 66	88.4
Hour 336	695 ± 286	71.5

n.a. = not applicable
SD = standard deviation calculated from replicate incubation bottles
% Loss = [100 – (total alkanes at the sampling hour/total alkanes at hour 0)] × 100

Table 2: Loss rate between each sampling point during the time series experiment

Time Periods	**Total Loss Rate (ppm/hr)**
Hour 0-6	222
Hour 6-12	116
Hour 12-24	5
Hour 24-48	1
Hour 48-168	Below detection
Hour 168-336	Below detection

Table 3: The total concentration of LMW and HMW alkanes and their percent loss at each sampling time during the time series experiment

Sample	LMW Alkanes (Mean ppm in sediments ± SD)	% Loss (Mean)	HMW Alkanes (Mean ppm in sediments ± SD)	% Loss (Mean)
Hour 0	1260 ± 302	n.a	1184 ± 294	n.a.
Hour 6	549 ± 172	56.3	558 ± 159	52.8
Hour 12	131 ± 79	89.5	279 ± 260	76.4
Hour 24	152 ± 131	87.9	194 ± 158	83.6
Hour 48	147 ± 151	88.3	160 ± 152	86.4
Hour 168	117 ± 26	90.6	165 ± 40	86.0
Hour 336	316 ± 135	74.8	378 ± 151	68.0

n.a = not applicable
SD = standard deviation calculated from replicate incubation bottles
% Loss = [100 – (total alkanes at the sampling hour / total alkanes at hour 0)] × 100

Table 4: Loss rate of LMW and HMW alkanes over the course of the time series experiment

Time Periods	LMW Loss Rate (ppm/hr)	HMW Loss Rate (ppm/hr)
Hour 0-6	98	85
Hour 6-12	90	65
Hour 12-24	below detection	7
Hour 24-48	below detection	1
Hour 48-168	below detection	below detection
Hour 168-336	below detection	below detection

Table 5: Values for normal alkane C_{17}:Pristane and normal alkane C_{18}:Phytane ratios over the course of the time series experiment

Sample	n-C17:PR	n-C18:PH
Hour 0	1.5	2.1
Hour 6	1.4	2.1
Hour12	1.1	1.4
Hour 24	1.1	1.4
Hour 48	1.1	1.4
Hour 168	2.5	2.9
Hour 336	1.2	1.5

3.2.2 PAH LOSS WITH TIME

During the time series experiment the following PAHs were identified: Naphathalene, 2-Bromonaphthalene, Acenaphthene, Fluorene, Fluoranthene, and Pyrene. Total PAHs showed substantial decreases during the first six hours of the experiment (Fig. 3, Table 6). By 6 hours 90.1% of PAHs were lost, and by 12 hours PAH concentrations increased slightly so that 63.6% PAHs were lost at the end of experiment (Table 6).

The LMW PAH compounds, including Naphthalene, 2-Bromonaphthalene and Acenaphthene, and Fluorene showed similar decreasing trends (Fig. 3). At hour 0, Naphthalene had the highest concentration of all PAHs, 8021 ppb, while 2-Bromonaphthalene and Acenaphthene and Fluorene had concentrations lower by one order of magnitude, which were 583 and 2130 ppb, respectively (Table 6). The majority of LMW PAHs (> 74%) loss occurred within the first 6 hours of the time series, and the Naphthalene had the highest %loss among all LMW PAH compounds. By hour 48 Naphthalene was decreased 87.2%, 2-Bromonaphthalene and Acenaphthene 69.8%, and Fluorene 82.7% (Table 7).

Unlike the alkane loss, we did not simulate the PAH loss with the multi-G model because of the consistently low RSQ values of fitting this model over the course of the experiment (RSQ=0.16 for first 48 hours and 0.02 for the whole experimental period).

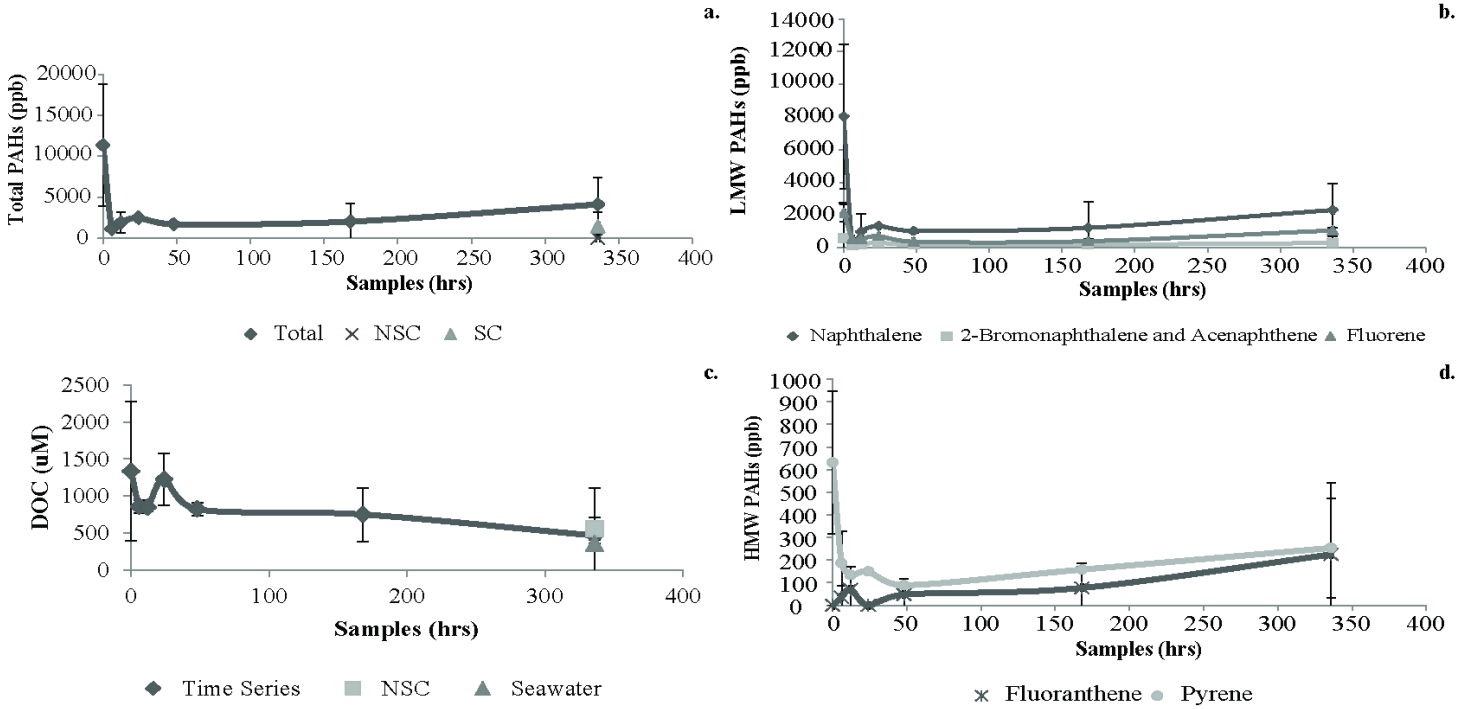

Figure 3: Changes in the concentrations of a) total PAH, b) LMW PAH, c) DOC, and d) HMW PAH over the course of the time series experiment. Error bars represent the SD of data from duplicate incubation bottles.

Table 6: Values of total, LMW, and HMW PAHs during the time series experiment

		LMW (ppb in sediments)			HMW (ppb in sediments)	
Sample	**Total (Mean ± SD)**	**Naphthalene (Mean ± SD)**	**2-Bromonaphthalene and Acenaphthene (Mean ± SD)**	**Fluorene (Mean ± SD)**	**Fluoranthene (Mean ± SD)**	**Pyrene (Mean ± SD)**
NSC (non-oiled)	3 ± 4	below detection	below detection	below detection	1 ± 2	1 ± 2
Hour 0	11366 ± 7452	8021 ± 4415	583 ± 541	2130 ± 2176	below detection	631 ± 315
Hour 6	1122 ± 106	228 ± 298	126 ± 47	545 ± 362	35 ± 50	186 ± 140
Hour 12	1914 ± 1319	972 ± 1081	191 ± 85	545 ± 42	71 ± 99	134 ± 9
Hour 24	2499	1331	307	711	below detection	150
Hour 48	1704 ± 211	1024 ± 105	175 ± 17	367 ± 26	47 ± 67	89 ± 5
Hour 168	2031 ± 2192	1214 ± 1622	183 ± 144	398 ± 327	77 ± 109	158 ± 11
Hour 336	4126 ± 3261	2304 ± 1631	287 ± 140	1055 ± 951	224 ± 318	253 ± 219

SD = standard deviation calculated from replicate incubation bottles

Table 7: Percent loss for total, LMW, and HMW PAHs during the time series experiment

		LMW			HMW	
Sample	**Total (%)**	**Naphthalene (%)**	**2-Bromonaphthalene and Acenaphthene (%)**	**Fluorene (%)**	**Fluoranthene (%)**	**Pyrene (%)**
Hour 0	n.a	n.a	n.a	n.a	n.a	n.a
Hour 6	90.1	97.1	78.3	74.4	n.a	70.5
Hour 12	83.1	87.8	67.1	74.4	-98.1	78.7
Hour 24	78.0	83.4	47.1	66.6	100	76.2
Hour 48	85.0	87.2	69.8	82.7	-34.0	85.8
Hour 168	82.1	84.8	68.6	81.2	-116.4	74.9
Hour 336	63.6	71.2	50.6	50.4	-531.1	59.8

n.a = not applicable
% Loss = [100 – (total alkanes at the sampling hour / total alkanes at hour 0)] × 100

In contrast, the two HMW PAHs, Fluoranthene and Pyrene, were not decreased similarly (Fig. 3). The initial concentration of Pyrene was 631 ppb, demonstrating a trend similar to LMW PAHs. The majority of Pyrene, 70.5%, was lost in the first 6 hours, and 85.8% of total amount was lost by hour 48 (Table 7). Fluoranthene was however not detected initially or at 24 hours but measured between 47 to 224ppb from hour 48 to 336 (Table 6).

3.2.3 AQUEOUS PHASE: INORGANIC NITROGEN, PHOSPHATE AND DOC

Nitrate+nitrite concentrations ranged from 6.8 – 51.5 µM, in which Nitrite only accounted for a small proportion and varied from 0.4 – 1.0 µM (Table 8). Ammonium ranged between 305.5 and 536 µM whereas Orthophosphate was from 0.1 and 4.3 µM (Table 8). None of these four nutrients showed consistently increasing or decreasing trends over time (Fig. 4). DOC concentrations ranged from the initial concentration of 1336.2 µM to the final concentration of 466.2 µM (Table 8), showing an overall decreasing trend throughout the time series experiment (Fig. 3, Table 8). The final concentration was comparable to the concentration in non-oiled seawater.

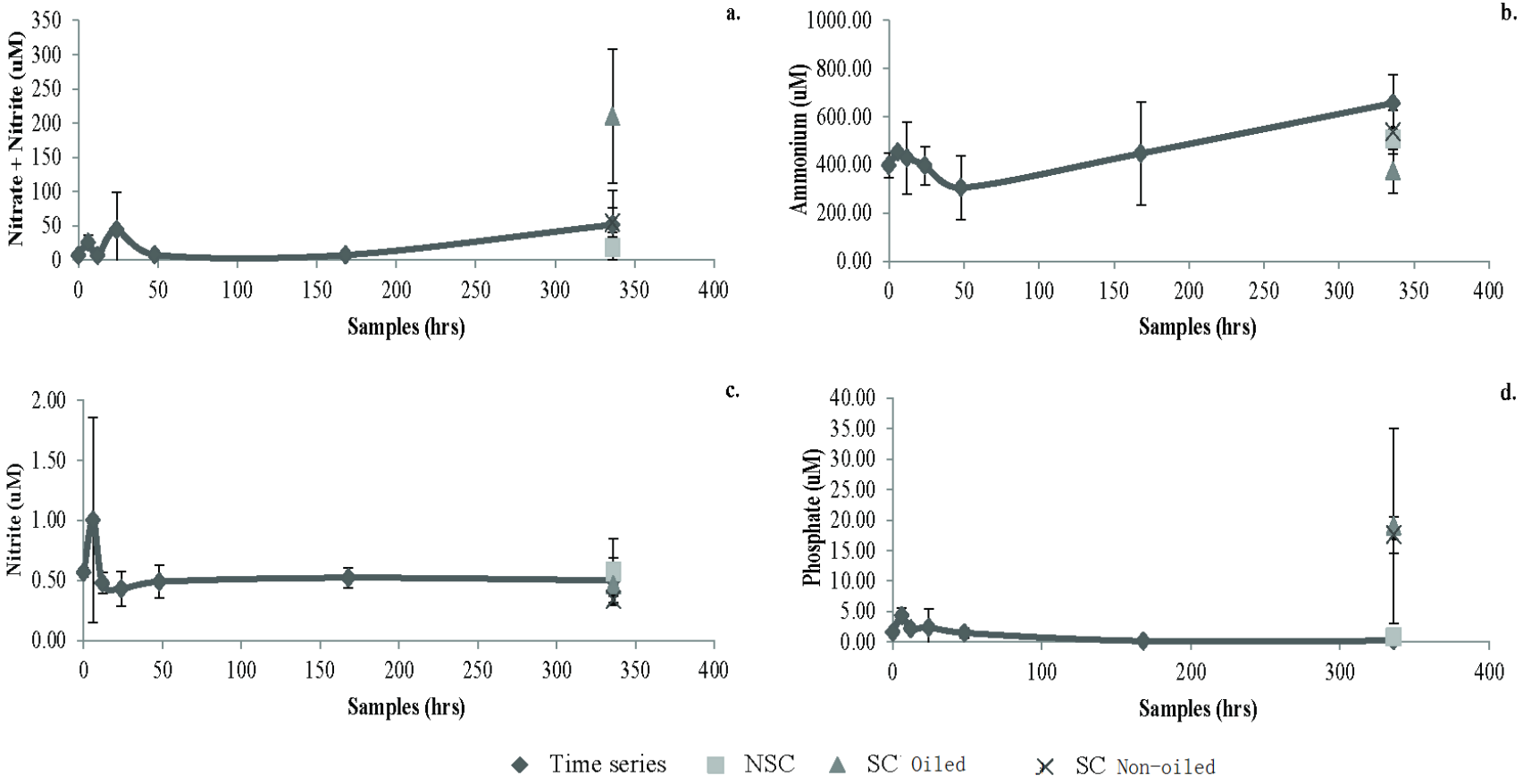

Figure 4: The changes in the concentrations of a) aqueous nitrate + nitrite, b) aqueous ammonium, c) aqueous nitrite, and d) aqueous phosphate over the course of the time series experiment. Error bars represent the SD of data from duplicate incubation bottles.

Table 8: The concentration of inorganic aqueous species and DOC over the course of the time series experiment

Sample	**Nitrate+Nitrite (uM) (Mean ± SD)**	**Nitrite (uM) (Mean ± SD)**	**Ammonium (uM) (Mean ± SD)**	**Phosphate (uM) (Mean ± SD)**	**DOC (uM) (Mean ± SD)**
NSC (non-oiled)	18.6 ± 21.3	0.5 ± 0.2	506.0 ± 40.9	0.8 ±0.6	561.0 ± 150.0
SC (oiled)	209.8 ± 97.8	0.4 ± 0.1	374.4 ± 90.9	19.0 ± 16.0	18008.9
SC (non-oiled)	54.7 ± 21.3	0.3 ± 0.0	536.4 ± 90.2	17.6 ± 3.0	9333.1 ± 12870.1
Hour 0	6.8 ± 3.9	0.5 ± 0.0	397.4 ± 50.9	1.6 ± 0.5	1336.2 ± 943.3
Hour 6	25.6 ± 11.1	1.0 ± 0.8	452.3 ±17.4	4.3 ± 1.1	857.3 ± 88.7
Hour 12	6.8 ± 1.9	0.4 ± 0.1	428.1 ± 150.1	2.1 ± 0.1	844.9 ± 50.9
Hour 24	44.1 ± 54.7	0.4 ± 0.1	396.8 ± 79.1	2.4 ± 3.1	1226.8 ± 353.8
Hour 48	7.8 ± 2.6	0.4 ± 0.1	305.5 ± 133.1	1.5 ± 0.8	822.5 ± 89.6
Hour 168	7.4 ± 1.1	0.5 ± 0.1	447.2 ± 212.6	0.1 ± 0.1	751.5 ± 363.1
Hour 336	51.5 ± 50.7	0.5 ± 0.1	655.9 ± 116.5	0.2 ± 0.1	466.2 ± 646.5

SD = standard deviation calculated from replicate incubation bottles

3.3 CONCENTRATION VARIATION EXPERIMENT

3.3.1 ALKANES

Non-sterile samples were compared to their sterile controls treated with the same amount of oil (Fig. 5). After 21 hour incubation, the oiled sterile controls had higher concentrations of alkanes than their non-sterile counterparts for 0.2g and 20g treatments, but had lower concentrations than the non-sterile counterparts for the 10g and 50g treatments (Table 9, Fig. 5). Non-sterile samples with 0.2g and 20g of oil contained ~83 and 94 % less alkanes than sterile counterparts, respectively (Table 9). The oiled SCs consisted of more than half of LMW alkanes, except the SC treated with 0.2g oil (SC-0.2g) in which 31% LMW alkanes were present (Table 10). All samples showed greater %HMW than the corresponding sterile controls (Table 10).

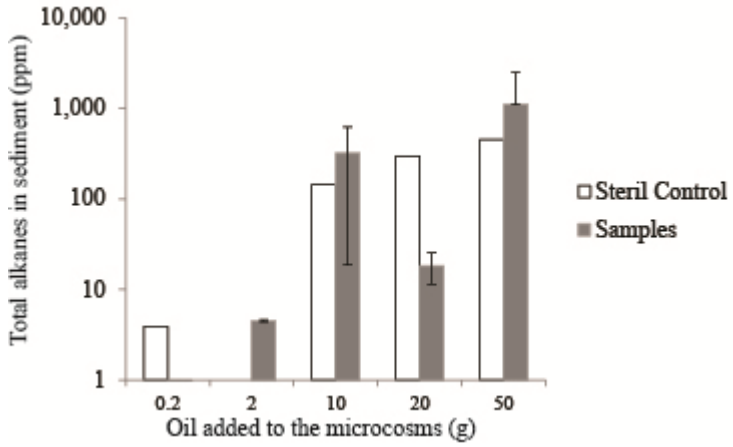

Figure 5: Comparison of total alkanes in sediments in samples and their sterile counterparts in the concentration variation experiments (error bars represent SD of duplicate bottles).

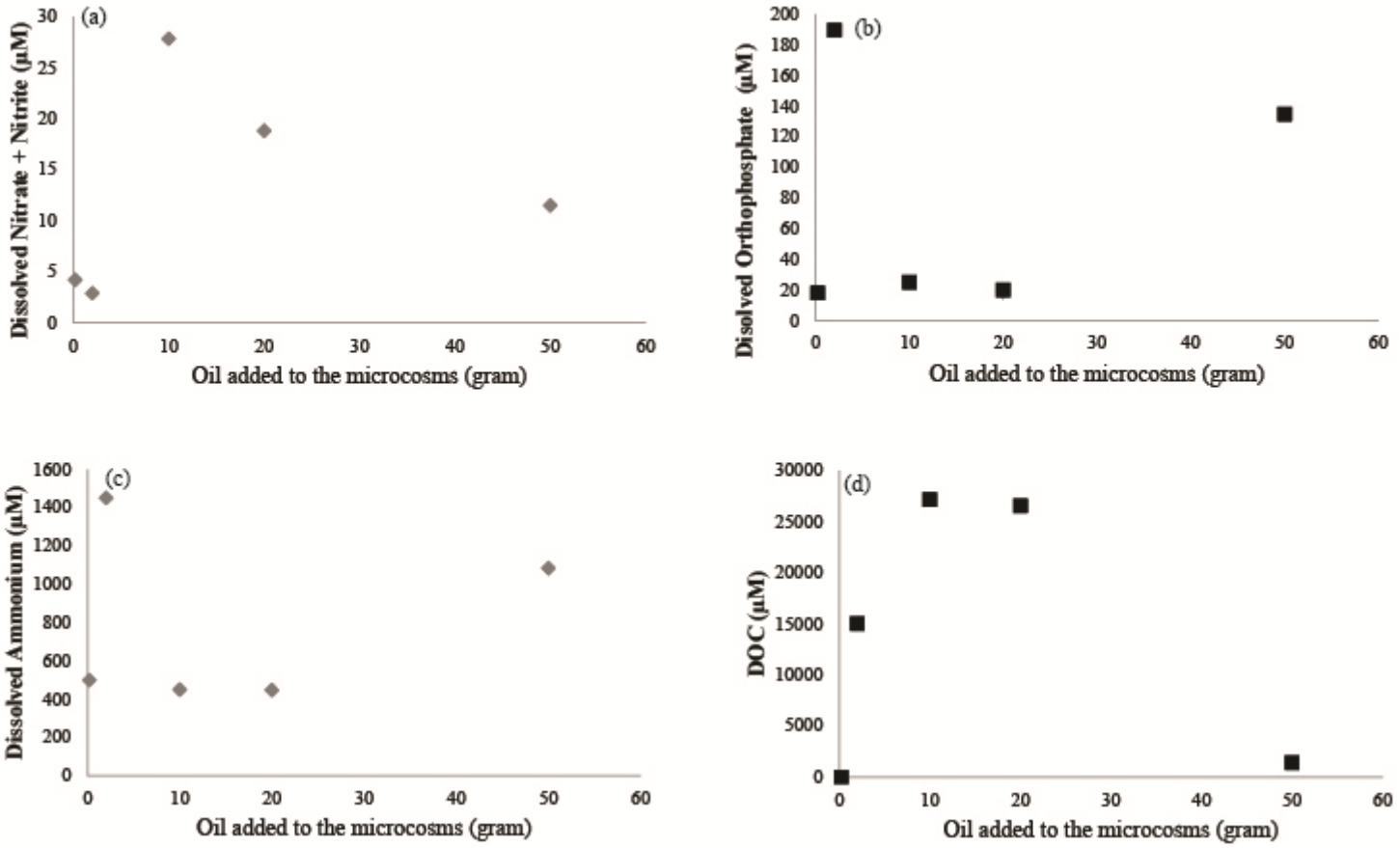

Figure 6: The concentration of oil added to each microcosm *vs.* the concentrations of dissolved nutrients and organic carbon for sterile controls samples in the concentration variation experiments.

Table 9: The concentration of total alkanes, LMW alkanes and HMW alkanes for the concentration variation experiment

Sample	Total (ppm) (Mean ± SD)	LMW (ppm) (Mean ± SD)	HMW (ppm) (Mean ± SD)
NSC (non-oiled)	below detection	below detection	below detection
SC-0g	below detection	below detection	below detection
SC-0.2g	3.9	1.2	2.7
SC-10g	144.1	81.1	62.9
SC-20g	296.4	161.7	134.6
SC-50g	454.6	262.5	192.1
0.2g	0.6 ± 0.2	0.1 ± 0.0	0.4 ± 0.1
2g	4.5 ± 0.1	1.5 ± 0.0	2.9 ± 0.1
10g	319.5 ± 300.8	175.2 ± 169.5	144.2 ± 131.2
20g	18.4 ± 7.0	7.1 ± 3.8	11.3 ± 3.2
50g	1098.1 ± 1398.0	614.9 ± 789.8	483.1 ± 608.1

SD = standard deviation calculated from replicate incubation bottles

Table 10: Percentage of LMW and HMW alkane distribution for samples in CV experiment

Sample	LMW (%)	HMW (%)
NSC (non-oiled)	n.a	n.a
SC-0g	n.a	n.a
SC-0.2g	31.1	68.8
SC-10g	56.3	43.6
SC-20g	54.5	45.4
SC-50g	57.7	42.2
0.2g	27.5	72.4
2g	34.5	65.4
10g	54.8	45.1
20g	38.6	61.3
50g	56.0	43.9

n.a = not applicable

3.3.2 AQUEOUS PHASE: INORGANIC NITROGEN, PHOSPHATE AND DOC

All aqueous nutrients showed no apparent trend with increasing oil concentrations (Fig. 6), indicating oil was not a source for these inorganic nutrients. Relative to their sterile counterparts, all samples had lower nitrate+nitrite content (Fig. 7, Table 11), indicating that these nutrients may be utilized by microbes during the 21-day incubation experiments. Such a pattern was however not observed for the concentration of dissolved phosphate and ammonium (Fig. 7).

DOC concentrations for both sterile controls and samples increased with oil concentration from 0-10 gram oil but decreased from 10-25 gram of oil (Fig. 6d). The sample treated with 0.2g and 50g of oil showed greater DOC values than their sterile counterparts, but the opposite pattern was found for samples treated with 2g, 10g and 20g of oil (Table 11, Fig. 8).

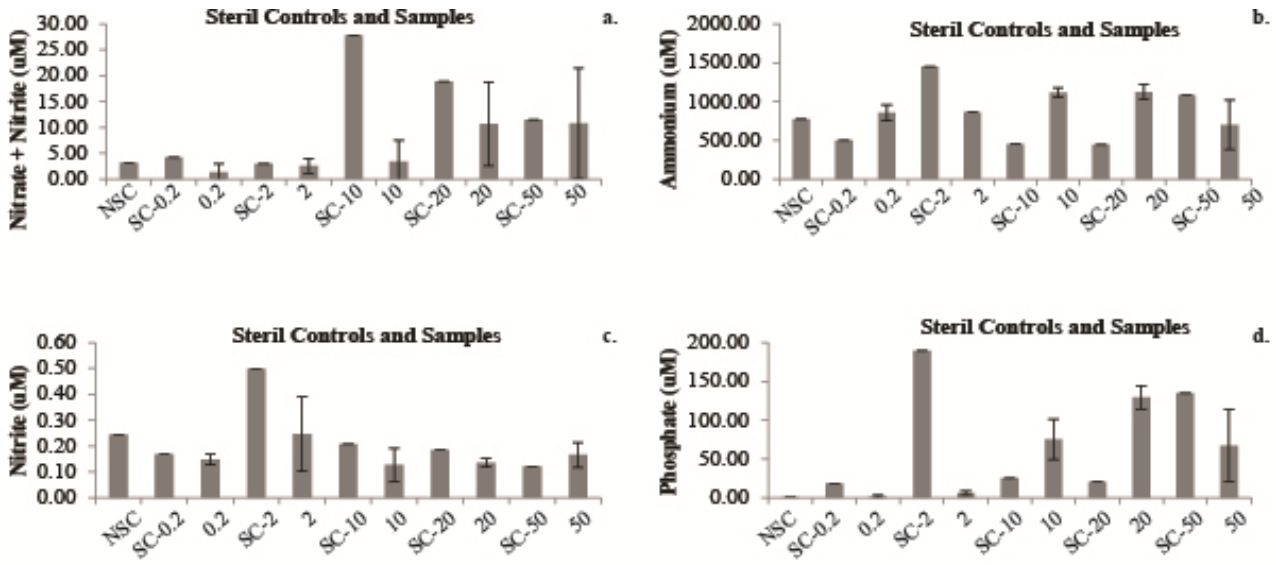

Figure 7: Comparison of aqueous inorganic N and P in samples and their sterile counterparts in the concentration variation experiments: (a) nitrate + nitrite (b) ammonium (c) nitrite (d) phosphate (error bars represent SD of duplicate bottles; 0.2, 2, 10, 20, 50 represents 0.2g, 2g, 10g, 20g and 50g of oil added to the microcosms respectively)

Table 11: The concentration of inorganic aqueous species and DOC for samples in the concentration variation experiment

Sample	Nitrate+Nitrite (uM) (Mean ± SD)	Nitrite (uM) (Mean ± SD)	Ammonium (uM) (Mean ± SD)	Phosphate (uM) (Mean ± SD)	DOC (uM) (Mean ± SD)
NSC (non-oiled)	3.1	0.2	770.4	0.6	455.1 ± 18.8
SC-0.2g	4.2	0.1	498.0	18.1	12.3
SC-2g	2.9	0.4	1449.5	189.6	15028.3
SC-10g	27.8	0.2	448.5	25.2	27159.1
SC-20g	18.8	0.1	445.8	20.1	26551.3
SC-50g	11.5	0.1	1082.0	134.9	1421.2
0.2g	1.3 ± 1.7	0.1 ± 0.0	852.6 ± 102.1	1.6 ± 1.8	731.1 ± 19.0
2g	2.5 ± 1.4	0.2 ± 0.1	860.4 ± 1.2	6.1 ± 2.9	647.1 ± 60.6
10g	3.4 ± 4.1	0.1 ± 0.1	1111.6 ± 61.7	75.4 ± 25.9	1251.4 ± 239.0
20g	10.6 ± 8.1	0.1 ± 0.0	1123.1 ± 90.1	129.0 ± 14.8	1395.0 ± 91.3
50g	10.7 ± 10.6	0.1 ± 0.0	699.3 ± 317.5	67.0 ± 46.0	12612.5 ±16215.4

n.a = not applicable
SD = standard deviation calculated from replicate incubation bottles

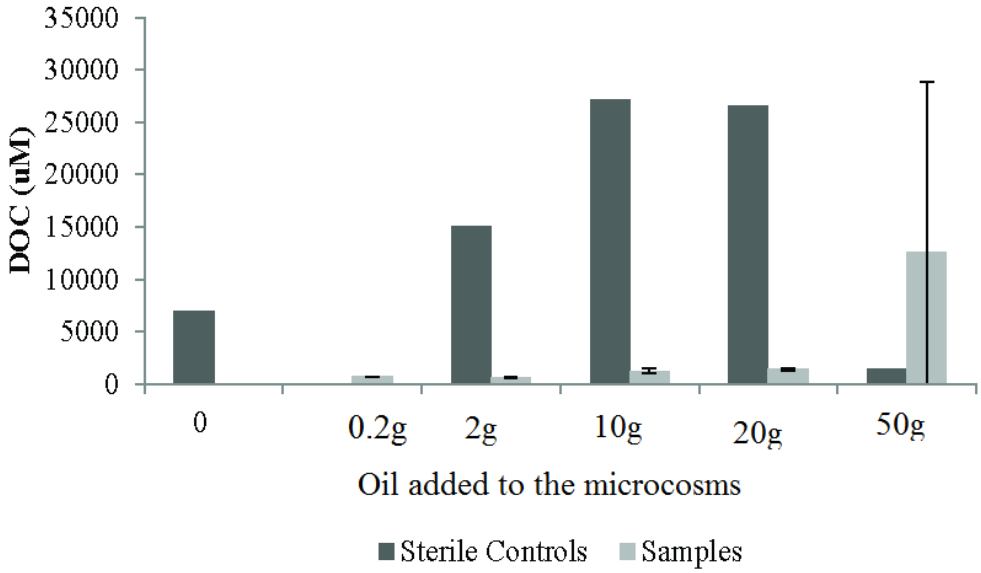

Figure 8: Comparison of aqueous DOC concentration between samples and sterile controls (error bars represent SD of duplicate bottles).

CHAPTER 4

DISCUSSION

4.1 TIME SERIES EXPERIMENT: THE % RECOVERY VALUES OF THE ALKANES IN SEDIMENTS

Total alkanes measured 2450 ppm (i.e., μg/g wet sediment) for the Hour 0 sample of the time series experiments (Table 1, Fig. 2). Because 326.94 g wet sediment was added to each microcosm (see method section), extractable saturated hydrocarbons in the sediment of the microcosm were calculated as 2450 ppm *326.94 g = 80,1000 μg (801 mg). The Q4000 Virtual Oil Summary (2011) analyzed 7 Macondo oil samples using GC-FID, and concluded that the extractable $C_{9\text{-}31}$ saturated hydrocarbons averaged 98 mg/kg oil. Relative to the total extractable hydrocarbons added the microcosms, the percent recovery of saturated hydrocarbons in the sediments of the microcosms was calculated as: 801 mg extractable saturated hydrocarbons / (98 mg saturated hydrocarbon/kg oil * 10 g added oil)*100%=~80%.

The majority of saturated hydrocarbons were detected in the sediments, which agrees with our expectation given that the tendency of non-polar hydrocarbons partitioning greater towards organic matter in sediment particles than towards water (Wang et al., 2001). Using $C_{14}H_{30}$ as an example, the ratio of the concentration in the sediment to the concentration in water in our microcosms is approximately equal to 10^6 (calculated as %organic carbon in the sediments * K_{oc}=1%*1.724*K_{ow}; Kow=10^8 from Sangester, 1989).

Part of unrecovered saturated hydrocarbons may be dissolved in water, which was supported by the elevated DOC concentration in oiled microcosms than in non-oiled microcosms

(Table 8). However, this part of saturated hydrocarbon was insignificant relative to hydrocarbon sorbed to the sediments. For example, the DOC concentration of Hour 0 was higher than non-oiled control by 775 µM, which was equal to 9300 µg carbon in the microcosm, accounting for only ~0.9% of total mass of extractable hydrocarbon in the sediments. This observation is unsurprising given the low solubility of the non-polar hydrocarbons (note that non-polar hydrocarbons are major components of Macondo oil, Reddy et al., 2011). Using Brigg's (1981) equation:

$$\log WS = 1 - \log K_{ow}$$

where K_{ow} represents octanol–water partition coefficient and WS is water solubility, we calculated that the water solubility of C_{11}, C_{12}, C_{13} and C_{14} alkanes was 0.4508, 0.2699, 0.0507 and 0.0198 mg/L, respectively (K_{ow} from Abraham et al., (1994) and Coates et al., (1985)). Theoretically, the 173.06g seawater in the microcosms of the time series experiments can dissolve 78.0µg of C_{11} alkane, 46.7µg of C_{12} alkane, 8.8 µg of C_{13} alkane and 3.4 µg of C_{14} alkane, which were 3–4 orders of magnitude less than total extractable hydrocarbons (98,000 µg). This estimate also did not consider the partition of hydrocarbons between water and sediments, which will further lower the relative abundance of hydrocarbons in water as discussed above.

In contrast, the saturated hydrocarbons in oil slicks floating on the seawater of the microcosms may account for an important fraction of unrecovered hydrocarbons, given that the Macondo oil (~0.84g/cm^3) is lighter than seawater. Additionally, we also observed that oil adhered to the sides of the glass jars and the lids during the experiments. This part of oil may

also account for a significant proportion of unrecovered hydrocarbons. Bælum et al. (2012) found that in microcosms with seawater spiked with Macondo oil approximately 70% of the initial 100 ppm concentration sorbed to the sides of their glass jars. However, we did not quantify the hydrocarbons existing as oil slicks or sticking to the glass jars.

4.2 THE LOSS OF HYDROCARBONS IN SEDIMENTS WITH TIME

In the time series experiment, the majority of aliphatic alkanes and PAHs in sediments were lost within the first 12 hours and 6 hours, respectively (Figs. 2 and 3, Tables 1 and 8). This loss may be attributed to aerobic microbial degradation of hydrocarbons, beginning with dioxygenase enzymes inserting O_2 into the hydrocarbon structure and yielding CO_2 and H_2O (Atlas and Philp, 2005). The loss rate of aliphatic hydrocarbons decreased rapidly after 12 hours (Fig. 2, Table 2), while the loss rate of PAHs decreased after hour 6. This is perhaps accounted for by oxygen depletion within the sediment of the microcosms, so that aerobes could no longer efficiently metabolize oil using oxygen as the electron acceptor. Although the variation in oxygen concentration was not monitored during the TS experiment, the depletion of oxygen in the microcosm was indirectly supported by the changes in iron content in seawater in our microcosms, which was below detection from hour 0 to 48 and increased to 7 mg/L at hour 168 (Rentschler, 2013). In oxic environments with a pH > 5 iron is insoluble and exists as particulate Fe (III) (Kirchman, 2012). Bacteria release siderophores, a LMW chelator that specifically bind to iron, enabling microbes to use Fe (III) as an electron acceptor to degrade hydrocarbons (Kirchman, 2012). Gauglitz et. al. (2012) isolated *Vibrio* sp. from the Gulf of Mexico after the Deepwater Horizon oil spill, and observed the production of a suite of siderophores. Based on

these observations, reduction of Fe (III) to Fe (II) via bacterial production of siderophores could account for the increase in aqueous iron concentration. However, the loss rate via this microbial degradation pathway was below detection in our microcosms (Tables 2 and 4), indicating it was not a pathway in removing alkanes from sediments as efficiently as aerobic degradation over a short term.

Between the time hydrocarbon loss slowed and when dissolved iron concentration increased, other electron acceptors may take the place of oxygen during anaerobic degradation. The theoretical energy yield for electron acceptors utilized by microbes has the following order from highest to lowest: oxygen > manganese > nitrate > iron > sulfate > carbon dioxide (Kirchman, 2012). Although nitrate is associated with higher energy yields than iron, throughout our time series it did not decrease and its reduced product ammonium did not show an evident increasing trend (Fig. 4). Two explanations may account for this observation. First, concentration and chemical form of electron acceptors may be more important factors than theoretical energy yield, as shown by nitrate being responsible for a disproportionally low fraction of respiration globally in spite of its high energy yield (Kirchman, 2012). In oiled marsh sediment from Barataria Bay, Louisiana, the electron acceptors also did not follow the order of theoretical energy yield, with mixed electron acceptors (sodium sulfate and sodium nitrate) being first utilized and followed by sulfate and nitrate (Boopathy et al., 2012). Rentschler (2013) found that iron concentrations in the sediments used in our experiments range from 7550 – 8000 ppm. The high iron concentration compared to nitrate could have caused the use of iron as an electron acceptor over nitrate.

Second, it was possible that we did not detect the changes in the concentration of nitrate that are accessible to sediment microbes. Our microcosm is a heterogeneous system where nitrate was not evenly distributed among seawater and sediment. Because we combined aqueous phases before and after centrifuging sediments, we did not distinguish changes in nitrate in seawater and sediments. It is thus likely that nitrate accessible to sediment microbes were depleted before iron but this change was minor relative to nitrate concentration in seawaters and hence undetected.

Another common electron acceptor in coastal and marine waters is sulfate (Kirchman, 2012). In a concurrent trace metal study, Rentschler (2013) measured aqueous sulfate content in the microcosms used in the present study and found little change throughout the time series experiment. This finding, similar to our nitrate data, suggests either sulfate was not used as an electron acceptor despite its high concentration, which contrasts with Boopathy et. al. (2012) on oiled salt marsh sediments in Louisiana, or the changes in sulfates accessible to sediment microbes were not detected.

4.3 COMPARISON OF THE LOSS OF HYDROCARBONS WITH DIFFERENT STRUCTURES AND MOLECULAR WEIGHTS IN SEDIMENTS

4.3.1 STRAIGHT-CHAIN *VS* BRANCHED ALKANES

The ratios of n-C_{17}:Pristane and n-C_{18}:Phytane are indicative of the degree of weathering/biodegradation of fresh to mildly weathered crude oil (Wang et. al., 1999). These ratios are based on the observation that bacteria generally metabolize straight-chain alkanes faster than branched alkanes, and therefore more weathered oil has overall lower ratios than less weathered, fresher oil (Wang et. al., 1999). For example, Pristane and Phytane in both North

Slope and Macondo crude oil resist degradation better than normal alkanes (Hostettler and Kvenvolden, 1994; Bence et. al., 1996; Zhou et. al., 2013). In our samples, these two ratios showed no evident pattern in the time series experiment (Fig. 2). This could be due that *in situ* microbes have been adapted to degrade a variety of hydrocarbons and similarly degraded normal and branched alkanes in our samples. When microbial communities are exposed to hydrocarbons, genetic changes occur and the proportion of oil-degrading bacteria increases (Atlas and Atlas, 1991). Based on this, our results are not surprising due to the vast amount of natural oil seeps and oil drilling activities that take place within the GOM (MacDonald et. al., 1993). In contrast, in Prince William Sound where the preferential biodegradation of normal alkanes over branched alkanes was observed after the North Slope oil spill, natural oil seeps are scarce due to the highly metamorphosed sedimentary rocks in the region (Bence et. al., 1996).

4.3.2 LMW *VS* HMW COMPOUNDS

The loss rates and extents of aliphatic hydrocarbons differed with their chain-lengths and molecular weights. LMW alkanes were lost faster and to a greater extent than HMW alkanes throughout the time series experiment (Fig. 2, Tables 4 and 5). This finding agrees with Zhou et. al. (2013), in which preferential degradation of LMW *n*-alkanes was observed after 24 hours in microcosms filled with seawater and Macondo oil under both light and dark conditions. Similar pattern was also shown during the degradation of heavier North Slope crude oil, where LMW alkanes were degraded faster than HMW alkanes (Hostettler and Kvenvolden, 1994).

Likewise, the loss rates of PAHs were influenced by their molecular weights. We found LMW PAHs were lost much faster relative to HMW PAHs when aerobic microbial degradation

is the main degradation process (Fig. 3, Table 8). In fact, Napthalene, the compound of the lowest MW of all detected PAHs, demonstrated highest loss rates (Fig. 3, Table 9). Similarly Ke et. al. (2002) reported the preference of LMW PAHs over HMW PAHs in sediments from a mangrove swamp in Hong Kong after an oil spill. Zhou et. al. (2013) also observed biodegradation of Naphthalene was higher than other PAH compounds in microcosm incubations of the Macondo oil.

The preferential degradation of LMW hydrocarbons relative to HMW hydrocarbons observed here is consistent with the general sequence of the biodegradation of hydrocarbons, i.e., shorter carbon chains or less complex structures of hydrocarbons allow for easier access of microbes and thereby were degraded faster than their HMW counterparts (Volkman et. al., 1984; Hostettler and Kvenvolden, 1994; Reddy et. al., 2011; Kirchman, 2012). Related to this, the spilled Macondo oil may be degraded faster than heavier crude oil from spill accidents involving heavier crude oil (e.g. Hostettler and Kvenvolden, 1994).

4.4 LOSS OF HYDROCARBONS IN AQUEOUS PHASE

In oil-added microcosms, DOC concentrations were higher than those without oil addition (e.g., NSC) (Table 11), indicating that the Macondo oil increased DOC concentration in seawater. This may result from the soluble LMW aromatic hydrocarbons present in mildly degraded oil, such as naphthalene (Volkman et al., 1984). Similarly, Zhou et al. (2013) recorded DOC concentrations as high as 6 mg-C/L near the Macondo wellhead, where normal DOC values for the northern GOM are < 1 mg-C/L (Guo et al., 1994).

DOC displayed continuous loss until reaching the levels of non-oiled seawater (Fig. 2). This pattern was similar to the biodegradation pattern of DOC in oiled seawater (Zhou et al., 2013) and perhaps reflected that dissolved hydrocarbons can be continuously and quickly biodegraded in seawater. This behavior is different from the degradation trend of hydrocarbons in the sediments, which showed rapid loss only within the first 12 hours. The difference may reflect the heterogeneity of our seawater-sediment microcosms; that is, oxygen in seawater was abundant enough for aerobic degradation of DOC over the course of experiment whereas oxygen in sediments only sustained aerobic degradations for the first 12hrs. The microcosm heterogeneity emulates the field observations that oil pollutants in water columns were lost faster than oil in sediments because microbes living in water columns have access to more abundant oxygen than microbes near or in sediments (Bælum et. al., 2012; Zhou et. al., 2013).

4.5 PRESENT STUDY RESULTS *VS* PREVIOUS STUDIES RESULTS

The relative abundance of degradable alkanes and the degradation rate determined in the present study are of the same order of magnitude as most values reported from previous studies (Table 12). Boopathy et al. (2012) reported lower numbers of %degradable alkanes, 8.1% total petroleum hydrocarbons over 80 days, from incubating salt marsh sediment contaminated with 720 ppm Macondo oil from Southeast Louisiana. However, the Macondo oil in Boopathy et al. (2012) must have been degraded in water and sediments before the incubation. Boopathy et al. (2012) found that the hydrocarbons were made up of 38% alkanes and 27% PAHs, which was different from the “fresher” Macondo oil. The Macondo oil collected near the wellhead contained extractable hydrocarbons made up of 74% alkanes and 16% PAHs (Reddy et al.,

2011). Therefore, the components susceptible to biodegrdation, particularly LMW alkanes may have been lost before the incubation in Boopathy et al. (2012), leading to the lower values for %degradable hydrocarbons relative to our result and other studies (Table 12).

Naphthalene loss percentage and rate observed in the present work is comparable to previous studies (Table 15). Heitkamp et al. (1987) measured naphthalene degradation in sediment from three freshwater lakes spiked with naphthalene. In Lin et al. (2010) and Balachandrana et al. (2012), naphthalene was added to cultured media in order to measure laboratory naphthalene degradation. The percentage loss of naphthalene from these previous studies is comparable to the present study whereas the loss rate of the naphthalene loss rate is double (Balachandrana et al., 2012) and triple (Lin et al., 2010) that of the present study (Table 15).

The degradation rates of total PAH found in our work were also consistent with previous findings that PAH biodegradation can be quite significant with the presence of sediment microbes. Xia et al (2006) incubated riverine water with different PAH compounds and found that the majority of chrysene, benzo(a)pyrene and benzo(g,h,i)perylene can be degraded within 20 days under the influence of sediment microbes. They further noted that degradation rates may be further enhanced by high sediment contents. Their finding suggests that sediment microbes are effective degraders of PAH compounds, which agrees with our observation that the majority of initially detected PAH in sediments were gone with time.

Table 12: Comparison of hydrocarbon loss values from literature to the current study

Study system	Oil type	Hydrocarbon loss (%)	Hydrocarbon loss rate (%·day $^{-1}$)	Source
Salt marsh sediment Alabama, USA	Macondo oil	88.4*	6.3	Present study
GOM seawater	Macondo oil	25**	5	Bælum et al. (2012)
Salt marsh sediment Louisiana, USA	Macondo oil	8.1**	0.10	Boopathy et al. (2012)
Estuarine sediment Lima River Estuary, Portugal	Arabian Light	32***	2.10	Almeida et al. (2013)

* quantified by total alkanes by using GC-FID; ** quantified by total petroleum hydrocarbons by using GC-FID; *** quantified by total petroleum hydrocarbons by Fourier transformed infrared spectroscopy

Table 13: Comparison of naphthalene loss values from literature to the current study

Study system	Oil type	Naphthalene loss (%)	Naphthalene loss rate (%·day $^{-1}$)	Source
Salt marsh sediment Alabama,USA	Macondo oil	97.1*	6.9	Present Study
Lake sediments-Arkansas; estuary sediment-Texas, USA	Naphthalene only	70**	1.7 - 2.9	Heitkamp et al. (1987)
Oil contaminated sediment Chetpet, India	Diesel oil, Naphthalene	99.14**	14.2	Balachandrana et al. (2012)
Cultured medium from oil refining wastewater sludge Fuzhou, China	Naphthalene only	99.1**	24.8	Lin et al. (2010)

* quantified by naphthalene using GC-MS; ** quantified by naphthalene using GC

4.6 CONCENTRATION VARIATION EXPERIMENTS

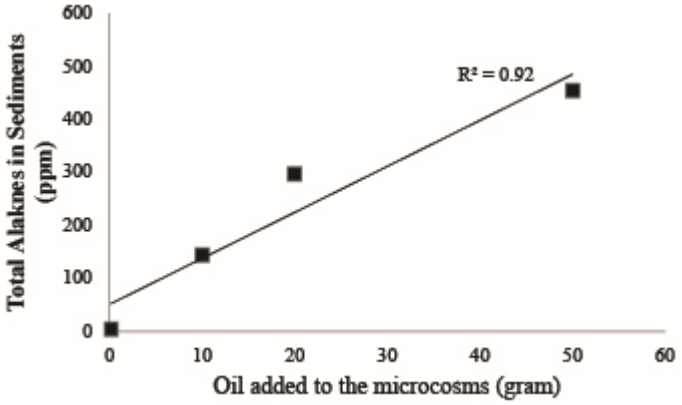

Figure 9: The concentration of oil added to each microcosm *vs.* the concentrations of total alkanes in the sediments of the sterile controls in the concentration variation experiments.

For the concentration experiment, the amount of alkanes in sediments increased with the amount of oil added to the microcosms in sterile controls (Fig. 9). The percent recovery rate of hydrocarbons in sediments was calculated the same as described in section 4.1, yielding recovery rate as 56%, 43%, 41% and 26% for 0.2g, 10g, 20g, and 50g of oil respectively.

It is possible that the values of %recovery were underestimated because the data from the reference sample, Q4000 Virtual Oil, were collected by conducting oil collection and oil extraction on the same day. In the current study, it took ~50 days for the Macondo oil to be transported to our laboratory since the collection. The Macondo oil was then stored at 4℃ for 4 days before the time series experiment and for additional 6 months before the concentration variation experiment. It is well likely that part of oil has been degraded before the experiment. This postulation is supported by %recovery in the concentration variation experiment being consistently lower than %recovery in the time series experiments. In addition, unlike the time

series experiment, the recovery rate for the concentration variation experiment was calculated based on the sterilized samples. The autoclave process to create sterilized samples may break down hydrocarbons at high temperatures and pressures and further lower the recovery rates of hydrocarbons in sediments.

The inner sphere surface complex that would form between hydrocarbon-organic matter, hydrocarbon-mineral surface, and organic matter-mineral surface can be quite complex and may be an ionic or covalent bond (Krauskopf and Bird, 2003). Although previous research has demonstrated that for a given sediment/soil type the sorption of neutral organic compounds may be generally correlated with the organic carbon contents in soil/sediment (Lambert, 1966, 1967, 1968), the amounts of hydrocarbons sorbed to sediments may vary greatly with sediment physical properties (e.g., grain size) and chemical variables (e.g, pH, ionic strength) (Karickhorf et al., 1978; Krauskopf and Bird, 2003; Johnsen et al., 2005). Given the sediment heterogeneity and the variability of pH and the concentrations of inorganic ions among the microcosms (Rentschler, 2013), it is unsurprising that the %recovery of hydrocarbons was variable for SC-0.2g, 0.2g, 10g, 20g, and 50g of the CS experiments (Fig. 9).

With the highly variable rates of %recovery, it is difficult to assess the importance of microbes in degrading hydrocarbons in the microcosms. In fact, even assuming that the %recovery rate was consistent for sterilized and non-sterilized microcosms treated with the same amount of oil, inconsistent conclusions were drawn on the importance of microbes in degrading hydrocarbons. Results from the concentration variation experiment for oil concentrations of 0.2g and 20g of oil support that microbes may play a role in degrading alkanes in the sediments (Fig.

5), i.e., oil concentrations were much higher after 21-day incubation by removing the microbial community, but the samples treated with oil concentrations of 10g and 50g of oil showed otherwise (Fig. 5). This uncertainty of alkanes in the sediments was echoed by the DOC concentration in the concentration variation experiment, which was higher in non-sterile samples for 0.2g and 50g of oil treatments but was higher in sterile controls for 2g, 10g and 20g of oil treatments (Fig. 8). Therefore, results from the concentration variation experiment provided inconclusive evidence of the importance of microbes in degrading hydrocarbons in the sediments and seawater.

CHAPTER 5

CONCLUSIONS

Due to the scarcity of data concerning the fates of Macondo oil after it arrived to Alabama coastal environments, the objective of the present study was to better understand the potential loss of Macondo oil derived hydrocarbons in Alabama salt marsh sediments and the associated regulating environmental factors. Several major findings of the present study are:

1. During the time series experiments, microbial degradation played an important role in degrading hydrocarbons in sediments. Oxygen availability was the main limiting factor for the rates and extents of microbial degradation of hydrocarbons. With the access of oxygen, microbes degraded hydrocarbons in water and sediments within hours. During anaerobic respiration, the degradation rates were much lower or even below detection.
2. The availability of hydrocarbons for microbial degradation depended on its structures and molecular weights. HMW PAHs were more persistent than LMW PAHs and HMW alkanes were more persistent than LMW alkanes. However, there was no preferential degradation of normal alkanes over branched alkanes.
3. Results from the concentration variation experiments did not provide conclusive evidence supporting that microbes play an important role in degrading hydrocarbons in the sediments. This lack of conclusive evidence may be due to high variability among microcosms associated with our environmental designs.

These findings improve the understandings of the fate of Macondo oil after it arrives in Alabama coastal sediments, providing direct evidence that crude oil may be rapidly degraded in

Alabama salt marsh sediments when it is in direct contact with oxygen. More research is needed to understand the persistence of oil compounds in low-oxygen environments over a longer period of time.

REFERENCES

Abraham, M.H., Chadha, H.S., Whiting, G.S., Mitchell, R.C. (1994). Hydrogen bonding. 32. An analysis of water-octanol and water-alkane partitioning and the Δlog p parameter of seiler. *Journal of Pharmaceutical Sciences, 83*(8), 1085-1100

Almeida, R., Mucha, A., Teixeira, C., Bordalo, A., Almeida C. (2013). Biodegradation of petroleum hydrocarbons in estuarine sediments: metal influence. *Biodegradation, 24*, 111-123

Alpkem Manual (1988). Alpkem Corporation, Clakamas, OR

Arzayus, K.M., Dickhut R.M., Canuel E.A. (2002). Effects of physical mixing on the attenuation of polycyclic aromatic hydrocarbons in estuarine sediments. *Organic Geochemistry, 33*(7)

Atlas R.M., and Atlas, M.C. (1991). Biodegradation of oil and bioremediation of oil spills. *Current Opinion in Biotechnology, 2*, 440-443

Atlas, R. M., & Hazen, T. C. (2011). Oil biodegradation and bioremediation: a tale of the two worst spills in U.S. history. *Environmental science & technology, 45*(16), 6709-15. doi:10.1021/es2013227

Atlas, R.M., and Philp, J. (2005). Bioremediation: Applied Microbial Solutions for Real-World Environmental Cleanup. ASM Press, American Society for Microbiology, 1752 N Street, N.W. Washington D.C. 20036-2904

Balachandran, C., Duraipandiyan, V., Balakrishna, K., Ignacimuthu, S. (2012). Petroleum and polycyclic aromatic hydrocarbons (PAHs) degradation and naphthalene metabolism in *Streptomyces* sp. (ERI-CPDA-1) isolated from oil contaminated soil. *Bioresource Technology, 112*, 83-90

Banjoo, D.R., and Nelson, P.K. (2005). Improved ultrasonic extraction procedure for the determination of polycyclic aromatic hydrocarbons in sediments. *Journal of Chromatography A, 1066*, 9-18

Bælum, J., Borglin, S., Chakraborty, R., Fortney, J.L., Lamendella, R., Mason, O.U., Auer, M., Zemla, M., Bill, M., Conrad, M.E., Malfatti, S.A., Tringe, S.G., Holman, H., Hazen, T.C., Jansson, J.K. (2012). Deep-sea bacteria enriched by oil and dispersant from the Deepwater Horizon spill. *Environmental Microbiology, 14*(9), 2405-2416

Bence, A.E., Kvenvolden, K.A., Kennicutt II, M.C. (1996). Organic geochemistry applied to environmental assessments of Prince William Sound, Alaska, after the *Exxon Valdez* oil spill – a review. *Organic Geochemistry, 24*(1), 7-42

Berner, R.A. 1964. An idealized model of dissolved sulfate distribution in recent sediment. *Geochim. Comochim. Acta* 28: 1497-1503

Geochim. Comochim. Acta 28: 1497-1503 Boopathy, R., Shields, S., Nunna, S. (2012). Biodegradation of crude oil from the BP oil spill in the marsh sediments of southern Louisiana, USA, *Applied Biochemistry and Biotechnology 167*, 1560-15

Briggs, G.C. (1981). Theoretical and experimental relationships between soil adsorption, octanol-water partition coefficients, water solubilities, bioconcentration factors, and the parachor, *Journal of Agricultural and Food Chemistry, 29*, 1050-1059

Coates, M., Connell, D.W., Barron, D.M. (1985). Aqueous solubility and octan-1-ol-water partition coefficients of aliphatic hydrocarbons. *Environmental Science and Technology, 19*(7), 628-632

Countway, R.E., Dickhut, R.M., Canuel, E.A. (2003). Polycyclic aromatic hydrocarbon (PAH) distributions and associations with organic matter in surface waters of the York River, VA Estuary. *Organic Geochemistry, 34*, 209-224

Ezra, S., Feinstein, S., Pelly, I., Bauman, D., Miloslavsky, I. (2000). Weathering of fuel oil spill on the east Mediterranean coast, Ashdod, Israel. *Organic Geochemistry, 31*(12), 1733-1741

Garrett, R. M., Pickering, I. J., Haith, C. E., Prince, R. C. (1998). Photooxidation of Crude Oils. *Environmental Science & Technology*, *32*(23), 3719-3723

Gauglitz, J.M., Zhou, H., Butler, A. (2012). A suite of citrate-derived siderophores from a marine *Vibrio* species isolated following the Deepwater Horizon oil spill. *Journal of Inorganic Biochemistry, 107*, 90-95

Guo, L., Coleman, C.H., Santschi, P.H. (1994). The distribution of colloidal and dissolved organic carbon in the Gulf of Mexico. *Marine Chemistry, 45*(1-2), 105-119

Heitkamp, M.A., Freeman, J.P., Cerniglia, C.E. (1987). Naphthalene biodegradation in environmental microcosms: estimates of degradation rates and characterization of metabolites. *Applied and Environmental Microbiology, 53*(1), 129-136

Hostettler, F.D. and Kvenvolden, K.A. (1994). Geochemical changes in crude oil spilled from the *Exxon Valdez* supertanker into Prince William Sound, Alaska. *Organic Geochemistry 21*(8/9), 927-936

Irwin, R.J. (1997). Environmental Contaminants Encyclopedia entry on Alkyl PAHs (Alkyl Homologs of PAHs. *National Park Service Water Resources Divisions, Water Operations Branch*

Johnsen, A.R., Wick, L.Y., Harms, H. (2005). Principles of microbial PAH-degradation in soil. *Environmental Pollution, 133*, 71-84

Ke, L., Wong, T.W.Y., Wong, Y.S., Tam, N.F.Y. (2002). Fate of polycyclic aromatic hydrocarbon (PAH) contamination in a mangrove swamp in Hong Kong following an oil spill. *Marine pollution bulletin*, *45*(1-12), 339-47

King, S.E., and Lester, J.N. (1995). The value of salt marsh as a sea defense. *Marine Pollution Bulletin*, *30*(3), 180-189

Kirchman, D.L. (2012) Processes in microbial ecology. *Oxford University Press*, 1st edition, Oxford, New York

Krauskopf, K.B. and Bird, D.K. (2003). Introduction to Geochemistry. *McGraw-Hill Publishing*, 3rd edition, ISBN-10: 0072918160

Lambert S. M. (1967) Functional relationship between sorption in soil and chemical structure. *Journal of Agriculture and Food Chemistry, 15*, 572-576.

Lambert S. M. (1966) The influence of soil-moisture on herbicidal response. *Weeds* 14, 273 275.

Lambert S. M. (1968) Omega (f~) a useful index of soil sorption equilibria. *Journal of Agriculture and Food Chemistry, 16(2)*, 340-343.

Leahy, J.G. and Colwell, R.R. (1990). Microbial degradation of hydrocarbons in the environment. *Microbiological Reviews, 54*(3), 305-315

Lin, C., Gan, L., Chen, Z.L. (2010). Biodegradation of naphthalene by strain *Bacillus fusiformis* (BFN). *Journal of Hazardous Materials, 182*, 771-777

MacDonald, I.R., Guinasso, N.L., Ackleson, S.G., Amos, J.F., Duckworth, R., Sassen, R., Brooks, J.M. (1993). Natural oil-slicks in the Gulf of Mexico visible from space. *Journal of Geophysical Research-Oceans, 98*, 16351-16364

Miralles, G., Nérini, D., Manté, C., Acquaviva, M., Doumenq, P., Michotey, V., Nazaret, S., Bertrand, J.C., Cuny, P. (2007). Effects of spilled oil on bacterial communities of mediterranean coastal anoxic sediments chronically subjected to oil hydrocarbon contamination. *Microbial ecology*, *54*(4), 646-61

Mitra, S., Lalicata, J.J., Allison, M.A., Dellapenna, T.M. (2009). The effects of Hurricanes Katrina and Rita on seabed polycyclic aromatic hydrocarbon dynamics in the Gulf of Mexico. *Marine Pollution Bulletin, 58*, 851-857

Natter, M., Keevan, J., Wang, Y., Keimowitz, A.R., Okeke, B.C., Son, A., Lee, M. (2012). Level and degradation of *Deepwater Horizon* spilled oil in coastal marsh sediments and pore-water, *Environmental Science and Technology, 46*, 5744-5755

Operational Science Advisory Team (OSAT-2), Gulf Coast Incident Management Team (2011). Summary report for fate and effects of remnant oil in the beach environment, http://www.restorethegulf.gov/release/2011/03/01/osat-2-fate-and-effects-oil-beaches

Oudot, J., and Chaillan, F. (2010), Pyrolysis of asphaltenes and biomarkers for the fingerprinting of the *Amoco-Cadiz* oil spill after 23 years, *Comptes Rendus Chimie, 13*, 548-552

Q4000 Virtual Oil Summary (2011), BP America Inc., BP Exploration & Production Inc., BP Gulf Coast Restoration Organization
(GCRO)

Reddy, C. M., Arey, J. S., Seewald, J. S., Sylva, S. P., Lemkau, K. L., Nelson, R. K., Carmichael, C. a, et al. (2011). Science Applications in the Deepwater Horizon Oil Spill Special Feature: Composition and fate of gas and oil released to the water column during the Deepwater Horizon oil spill. *Proceedings of the National Academy of Sciences of the United States of America*

Rentschler, E.K. (2013). Deepwater Horizon oil spill: using microcosms to study effects of crude oil in coastal sediments, M.S. thesis, University of Alabama

Risdon, G.C., Pollard, S.J.T., Brassington, K.J., McEwin, J.N., Paton, G.I., Semple, K.T., Coulon, F. (2008). Development of an analytical procedure for weathered hydrocarbon contaminated soil within a UK risk-based framework, *Analytical Chemistry, 80*(18), 7090-7096

Sangester, J. (1989) Octanol-water partition coefficients of simple organic compounds, *Journal of Physics and Chemistry Reference Data*, 18, 1111-1227.

Volkman, J.K., Alexander, R., Kagi, R.I., Rowland, S.J., Sheppard, P.N. (1984). Biodegradation of aromatic hydrocarbons in crude oils from the Barrow sub-basin of Western Australia, *Organic Geochemistry, 6*, 619-632

Wang, X., Zhang, Y., Chen, R.F. (2001). Distribution and partitioning of polycyclic aromatic hydrocarbons (PAHs) in different size fractions in sediments from Boston Harbor, United States. *Marine Pollution Bulletin, 42*(11), 1139-1149

Wang, Z., Fingas, M., Page, D. S. (1999). Oil spill identification. *Journal of Chromatography A, 843*(1-2), 369-411

Westrich, J.T., Berner, R.A. (1984). The role of sedimentary organic matter in bacterial sulfate reduction: The G model tested. *Limnology and Oceanography* 29: 236-249.

Wu, Y., Zhang, J., Mi, T-zhu, Li, B. (2001). Occurrence of n-Alkanes and polycyclic aromatic hydrocarbons in the core sediments of the Yellow Sea. *Marine Chemistry, 76*(1-2), 1-15

Xia, X.H., Yu, H., Yang, Z.F., Huang, G.H. (2006). Biodegradation of polycyclic aromatic hydrocarbons in the natural waters of the Yellow River: Effects of high sediment content on biodegradation. *Chemosphere, 65*, 457-466

Yamada, M., Takada, H., Toyoda, K., Yoshida, A., Shibata, A., Nomura, H., Wada, M., Nishimura, M., Okamoto, K., Ohwada, K. (2003). Study on the fate of petroleum-derived polycyclic aromatic hydrocarbons (PAHs) and the effect of chemical dispersant using an enclosed ecosystem, mesocosm. *Marine pollution bulletin, 47*(1-6), 105-13

Zhou, Z., Liu, Z., Guo, L. (2013). Chemical evolution of Macondo crude oil during laboratory degradation as characterized by fluorescence EEMs and hydrocarbon composition. *Marine Pollution Bulletin, 66,* 164-175